Contract No.:

This manuscript has been authored by Savannah River Nuclear Solutions (SRNS), LLC under Contract No. DE-AC09-08SR22470 with the U.S. Department of Energy (DOE) Office of Environmental Management (EM).

Porous iron material for TcO_4^- and ReO_4^- sequestration from groundwater under ambient oxic conditions

Dien Li[a,*], John C. Seaman[b], Simona E. Hunyadi Murph[a,c], Daniel I. Kaplan[a], Kathryn Taylor-Pashow[a], Renfei Feng[d], Hyunshik Chang[e], Madan Tandukar[e]

[a] Savannah River National Laboratory, Aiken, SC 29808, USA

[b] Savannah River Ecology Laboratory, University of Georgia, Aiken, SC 29802, USA

[c] Department of Physics and Astronomy, University of Georgia, Athens, GA 30602, USA

[d] Canadian Light Source, Saskatoon, SK S7N 0X4, Canada

[e] Höganäs Environmental Solutions LLC, Cary, NC 27513, USA

[*] Corresponding author.

Email: Dien.Li@srs.gov. (D. Li).

ABSTRACT: Technetium-99 (^{99}Tc) is a major contaminant at nuclear power plants and several US Department of Energy sites. Its most common aqueous species, pertechnetate (TcO_4^-), is very mobile in the environment, and currently there are no effective technologies for its sequestration. In this work, a porous iron (pFe) material was investigated for TcO_4^- and perrhenate (ReO_4^-) sequestration from artificial groundwater. The pFe was significantly more effective than granular iron for both TcO_4^- and ReO_4^- sequestration under oxic conditions. The Tc removal capacity was 27.5 mg Tc/g pFe at pH ~6.8, while the Re removal capacity was 23.9 mg Re/g pFe at pH ~10.6.

Tc K-edge XANES and EXAFS analyses indicated that the removed Tc species was 70-80% Tc(IV) that was likely incorporated into Fe corrosion products (i.e., Fe(OOH), Fe_3O_4) and 20-30% unreduced TcO_4^-. In contrast, the removed Re species was ReO_4^- only, without detectable Re(IV). In addition, the sequestered ReO_4^- was not extracted (<3%) by 0.1 M Na_2SO_4 and 1 M KI solution, which indicated that ReO_4^- and by chemical analogy, unreduced TcO_4^-, was likely incorporated into Fe corrosion products. This inexpensive pFe material may be applied to the sequestration and stabilization of $^{99}TcO_4^-$ from contaminated environments and nuclear waste streams.

Keywords: Pertechnetate, Perrhenate, porous iron, Synchrotron XANES and EXAFS

1. Introduction

Technetium-99 (^{99}Tc), a beta emitter ($\beta^- \approx 249$ keV), is a major long-lived ($t_{1/2} \approx 211{,}000$ years) fission product of uranium. Technetium contamination has been inadvertently introduced into the environment from leaks at nuclear waste storage facilities and currently is a key risk driver at several US Department of Energy (DOE) sites [1, 2]. Today, nuclear energy is considered one of the most feasible and economically sustainable clean energy resources in the foreseeable future. With the continued expansion of nuclear power throughout Asia, the ^{99}Tc-bearing nuclear waste stockpile is expected to grow [3]. Novel and practical technologies are needed for Tc sequestration and nuclear waste treatment to reduce its potential risk to the environment and living organisms.

The most common aqueous species of Tc is TcO_4^- [1, 2]. Currently, two general approaches for TcO_4^- immobilization are based on ion exchange or reduction. For example, strong base resins with quaternary amines have been used to remove TcO_4^-. However, the expensive resins

have demonstrated a modest TcO_4^- loading capacity from raffinate waste streams [4-6]. This is due to strong competition from other anions (e.g., NO_3^- and HCO_3^-) that are typically several orders of magnitude higher in concentration than TcO_4^- [4]. In the case of nuclear waste streams, chemical treatment methods that use reducing agents [7] or bacteria [8] are more effective for TcO_4^- immobilization [9]. Nevertheless, there are several disadvantages for such reductive technologies: 1) they are expensive as creation and maintenance of reducing environments are laborious and operationally complex [10]; 2) bioreduction processes require a steady supply of electron donors (e.g., acetate, ethanol, vegetable oil) for a sustained effectiveness [8, 11]; and 3) the solubility of the resulting $TcO_2 \cdot 1.6H_2O$ in groundwater ($\sim 1.5\times10^{-8}$ M) and in alkaline (e.g., pH ~13) cementitious material leachate ($\sim 1\times10^{-4}$ M) [12] greatly exceeds the Environmental Protection Agency (EPA) maximum contaminant level for ^{99}Tc (5.8×10^{-10} M or 900 picocuries per liter). Additionally, $TcO_2 \cdot 1.6H_2O$ can be readily re-oxidized and re-mobilized under most environmental conditions [13, 14].

Recent studies show that low solubility Tc sulfide phases are plausible for Tc sequestration and stabilization [15, 16]. TcO_4^- can be reduced forming a sulfide phase (e.g., Tc_2S_7 or TcS_2) by H_2S [17], amorphous iron sulfide [18], and abiotically sulfidized nano zero-valent iron [19]. Nevertheless, it has been observed that TcS_2 was transformed to TcO_2 after 120 h of oxidation [20]. In addition, TcO_4^- can be incorporated into the Fe(OOH) structure through reductive co-precipitation [21]. Because ReO_4^- has some similar aqueous chemistry properties to those of TcO_4^-, it is commonly used as a non-radioactive chemical analog for TcO_4^-. Several studies demonstrated that ReO_4^- can be incorporated into the sodalite structure [22, 23] and corroded steel [24]. However, these sequestration and stabilization methods were evaluated under well-controlled, specific laboratory conditions, and they have not been tested under field applications.

Zero valent iron (ZVI) is inexpensive and environmentally friendly. It is a commonly used reducing agent for chemical reactions in various environmental and industrial processes, including remediation of Cr, As, U, nitro-aromatic compounds and chlorinated organic solvents [25-29]. However, there are several limitations in the applications of conventional ZVI media to full-scale environmental remediation, due to surface passivation, change of ambient pH, high Fe leaching, low reactivity, and low selectivity caused by the presence of competing ions [30, 31]. In addition, there are few laboratory studies about ZVI applications for TcO_4^- or ReO_4^- removal [32-37]. Recently, a novel porous iron composite material was developed, which has increased surface area with enhanced reactivity [38, 39], but it has not been studied yet regarding its effectiveness for Tc sequestration from groundwater and other nuclear wastes.

The overarching objective of the present study was to investigate this newly developed porous iron composite (pFe) material for TcO_4^- sequestration and stabilization from contaminated groundwater and liquid nuclear waste streams. More specifically, we extensively characterized this pFe via a series of analytical techniques, including powder X-ray diffraction (XRD), scanning electron microscopy (SEM) and energy dispersive X-ray spectroscopy (EDS). The pFe material was further tested for its sequestration capability of TcO_4^- and ReO_4^- from artificial groundwater (AGW) under oxic conditions. Perrhenate (ReO_4^-) was chosen as a surrogate for TcO_4^-, because of their similar physiochemical properties (e.g., oxidation states, ionic radius, and energy of hydration) [1, 40], but it is noted that they have different redox potentials (E^0 = -0.548 V for ReO_4^- vs E^0 = -0.361 V for TcO_4^-) [36]. We also determined the chemical speciation of the sequestered Tc and Re and proposed mechanisms responsible for TcO_4^- and ReO_4^- removal using synchrotron Tc K-edge, Re L-edge and Fe K-edge X-ray

absorption near-edge structure (XANES) and extended X-ray absorption fine structure (EXAFS) spectroscopy.

2. Materials and methods

2.1 Materials

The porous iron (pFe) materials were provided by Höganäs Environmental Solutions (Cary, NC, USA). Ammonium pertechnetate (NH_4TcO_4) was purchased from Eckert & Ziegler Isotope Products (Valencia, CA, USA). Sodium sulfate (Na_2SO_4) and potassium iodide (KI) were purchased from Fisher Scientific (Hampton, NH, USA), while granular iron (gFe) and sodium perrhenate ($NaReO_4$) were purchased from Sigma-Aldrich (St. Louis, MO, USA). The chemicals were used as received. A known amount of NH_4TcO_4 was dissolved in AGW to prepare 3.2×10^{-4} M pertechnetate stock solution, while a known amount of $NaReO_4$ was dissolved in AGW to prepare 5×10^{-3} M perrhenate stock solution, which were used for batch sorption experiments. The composition of the AGW solution is typical uncontaminated groundwater from the Department of Energy's Savannah River Site (SRS), located near Aiken, South Carolina, USA [41]. The chemical composition (in mg/L) of the AGW was Na 1.25, K 0.25, Ca 0.93, Mg 0.66, Cl 5.51, and SO_4 0.73 and it had a pH of 6.3 ± 0.3 [42].

2.2. Material characterization

The pFe composite material was characterized by powder X-ray diffraction (XRD) analysis (Bruker D-2 Phaser) using Cu Kα radiation (λ = 1.5406 A) operating at 30 kV and 10 mA. The XRD data were collected at 2θ from 10° to 90°, with a 0.01° step and 2 seconds for each data point. The morphology and compositions of this pFe material were also characterized by Scanning Electron Microscope (SEM) coupled with Energy Dispersive X-Ray Spectroscopy

(EDS). To do this, the pFe sample was mounted on Al specimen stubs using double-sided carbon tape and imaged with a Hitachi SU8200. SEM images were collected at 20 kV at a working distance of 10 mm, while EDS data was collected at 15 kV and a working distance of 15 mm. Samples were stable and not affected when exposed to the electron beam. In addition, surface area and pore volume were measured by N_2 isotherms conducted at 77 K using a Micromeritics TriStar 3020. Pore size distributions were calculated using Non-Localized Density Functional Theory (NLDFT) and N_2 isotherms.

2.3. Batch adsorption experiments

Batch sorption experiments for obtaining the adsorption isotherms were conducted in an AGW surrogate under ambient atmosphere and temperature (22 °C). For each set of experiments, a sorbent-free control was included at the initial Tc concentration for q_e calculation and to provide an indication of Tc sorption to the reaction tube during the experiment. Approximately 0.01-0.05 grams of sorbent and a known volume of AGW were added to 15 mL polypropylene centrifuge tubes. Then, 0.05-5 mL of the Tc stock solution was added to make the final working solution volume of 5 mL with Tc concentrations ranging from 3.2×10^{-6} M (0.32 mg/L) to 3.2×10^{-4} M (32 mg/L). Given the high fission yield for Tc-99 and its long half-life (211,000 yrs), waste concentrations in the mg/L range are relevant to remediation scenarios. For example, the Tc-99 concentration in low level tank waste at the DOE Savannah River Site (SRS) is ~2 mg/L, while the highest Tc concentration measured in any of the SRS high-level waste tanks was ~84 mg/L [43]. The suspensions were equilibrated on a reciprocating shaker for 6 days, without pH adjustment. After equilibration, the final pH values were measured (Radiometer Copenhagen PHM 95 pH meter), and each suspension was filtered through 0.2 μm pore size nylon membrane syringe filters. The filtrate was analyzed for Tc by liquid scintillation counting (LSC) (LS 6500

Multi-Purpose Scintillation Counter, Beckman Coulter, Inc.) using Optiphase HiSafe (Perkin Elmer, Inc.) scintillation cocktail.

Similarly, to obtain Re isotherm curves, approximately 0.05 grams of the solid and a known volume of AGW were added to 15 mL polypropylene centrifuge tubes. Then, the AGW solution was spiked with an appropriate amount of 5×10^{-3} M $NaReO_4$ stock AGW solution so that the 5 mL working solution had a Re concentration ranging from ~5×10^{-5} to 5×10^{-3} M. The suspensions were equilibrated on a reciprocating shaker for 6 days, also without pH adjustment. The final pH values were measured, and each suspension was passed through 0.2 μm pore-size nylon membrane syringe filters. The filtrate was acidified for preservation (2% HNO_3) and analyzed for Re by inductively coupled plasma mass spectrometry (ICP-MS; NexION 300X, Perkin Elmer, Inc.) in accordance with the quality assurance and quality control protocols of EPA method 6020A [44].

Further, in order to better understand Re speciation and removal mechanisms, three-day extraction experiments for pFe samples after exposure to ReO_4^- were conducted using four procedures: 1) deionized water, 2) deionized water after one-minute Vortex agitation, 3) 0.1 M Na_2SO_4 solution, and 4) 1 M KI solution. Similarly, the extraction effluents were filtered and the Re concentrations were analyzed using ICP-MS.

2.4. Synchrotron XANES and EXAFS measurements

After the batch adsorption experiments, the solid samples were air dried and collected for spectroscopic characterization. Technetium K-edge XANES and EXAFS spectra of the pFe samples were collected using the Sector 20-BM beamline at the Advanced Photon Source (APS) (Argonne National Lab, Argonne, IL). To do so, 50 mg of each of the air-dried powder samples

was pressed into a 6.3-mm diameter disk pellet and sealed by Kapton tape. The APS sector 20-BM beam line employed a Si (111) double crystal monochromator detuned 15% for harmonic rejection. Additional harmonic rejection was provided by a Rh-coated mirror set at 2.8 mrad. Absolute energy calibration was made using a Mo foil with the edge energy of 20,000.4 eV. The APS storage ring was operated at 100 ± 5 mA during the measurements. The Tc K-edge XANES and EXAFS spectra were taken in fluorescence step-scanning mode using a 13-element Ge detector array at 90° to the beam direction, in the energy range of 20,850-22,013 eV at room temperature. The fluorescence detector had a four-layer Al foil filter to suppress the Fe fluorescence [24].

Rhenium L-edge and Fe K-edge XANES and EXAFS spectra were collected using the Canadian Light Source (CLS) Very Sensitive Elemental and Structural Probe Employing Radiation from a Synchrotron (VESPERS, 07B2-1) beamline (Saskatoon, SK, Canada). The VESPERS beamline is a hard X-ray microprobe beamline equipped with double crystal Si (111) and double multilayer monochromators [45]. The double crystal Si (111) monochromator was used to scan the photon energy for Re L-edge and Fe K-edge XANES and EXAFS measurements. The experiment was carried out using fluorescence mode, where the characteristic X-ray fluorescence from Re or Fe was collected by a Canberra 13-element Ge detector and the incident flux by a N_2-filled ionization chamber. The CLS storage ring was operated at 140-200 mA during the measurements.

All the collected spectra were processed and analyzed using the IFEFFIT software package including Athena and Artemis [46]. Data from multiple scans were processed using Athena by aligning and merging the spectra followed by background subtraction using the AUTOBK algorithm. Linear combination fitting to Tc and Fe K-edge XANES and EXAFS data in k space

were conducted using Athena. Rhenium L-edge EXAFS data analysis was conducted on the merged and normalized spectra using Artemis. Theoretical models were constructed with the program FEFF7 [32, 46]. Sodium perrhenate was used as a reference structural model [47]. Fits to the Re EXAFS data were made in R space (R from 1 to 3 Å) and obtained by taking the Fourier transform (FT) of χ(k) (k from 3 to 10) with a k weighting of 2.

3. Results and discussion

3.1. Characterization of pFe by powder XRD, SEM and EDS

Powder XRD pattern of the pFe material is shown in Fig. 1A. It consists of amorphous Fe and α-Fe that is characterized by three major diffraction peaks at 2θ = 45.1 (d = 2.01 Å), 67.2 (d = 1.39 Å) and 81.4 (d = 1.18 Å). The three peaks are indexed as (100), (200) and (211) of α-Fe, respectively. SEM imaging and EDS mapping were used to evaluate the morphology, pore structure, and composition of the pFe material. Its SEM images (Fig. 1B and 1C) show the wormlike and tubular-like pore structures throughout the entire pFe material. The pore morphologies vary in size and shape. Overall, the pore dimensions range around 1-3 μm with irregular and undefined shape. The EDS spectrum (Fig. 1D) shows that the pFe material is >92% Fe, and other observed impurities (i.e., C and Al) might be associated with the pFe material or the carbon tape and Al stub used for SEM imaging. In addition, the nitrogen sorption isotherm indicated that this pFe material has a BET surface area of 0.95 m^2/g, pore volume of 0.0068 mL/g, and average pore diameter of 364 Å.

3.2. Capacities of pFe for TcO_4^- and ReO_4^- sequestration

Batch adsorption experiments were conducted to compare the sequestration performance between pFe and gFe for TcO_4^- and ReO_4^- from AGW at equilibrium pH values. The mass of Tc or Re sorbed (q_e, mg/g) was calculated using equation 1:

$$q_e = \frac{(C_0 - C_e) \times V}{M} \quad (1)$$

where C_0 (mg/L) is the initial concentration in the control samples, C_e (mg/L) is the final concentration remaining in the solution, V is the volume of the solution (mL) and M is the mass of the sorbent (g). Fig. 2 shows that pFe was significantly more effective than gFe for the sequestration of both TcO_4^- and ReO_4^- from AGW under similar experimental conditions, most likely because the pFe has surface area of ~1 m^2/g, which is up to ~100 times higher than the surface area, typically 0.01 - 0.02 m^2/g, of conventional granular iron.

Further, the adsorption isotherms of TcO_4^- onto pFe after equilibration for six days under oxic conditions were obtained and are shown in Fig. 3. The Langmuir isotherm model (equation 2) was used to describe the data, as shown in the inset of Fig. 3:

$$\frac{C_e}{q_e} = \frac{1}{q_{max}} C_e + \frac{1}{K_L \times q_{max}} \quad (2)$$

where q_e is the mass of Tc sorbed onto pFe at equilibrium, q_{max} is the saturation sorption capacity, C_e is the Tc concentration in solution at equilibrium, and K_L is the Langmuir constant that is directly related to the binding site affinity. The obtained saturation capacity of pFe for TcO_4^- removal from AGW at the equilibrium pH value of ~6.8 was 27.5 mg Tc/g pFe. In addition, the Tc isotherm data were attempted to fit using Freundlich model (Fig. S1), which indicated that they were not well fitted using this model with a R^2 of 0.87.

Similarly, the adsorption isotherms of ReO_4^- onto pFe after equilibration for one day and six days under oxic conditions are shown in Fig. 4A. The Re adsorption isotherms for pFe appeared to approach their saturation. The Langmuir fits to the corresponding experimental data are shown in Fig. 4B. The adsorption isotherms for pFe were described well by the Langmuir model (R^2 >0.97). The obtained Re saturation capacities for pFe from AGW at the equilibrium pH values were 8.6 and 23.9 mg/g at day 1 and day 6, respectively. In addition, the Re isotherm data were attempted to fit using Freundlich model (Fig. S2), which indicated that the 6-day Re isotherm curve was also not well fitted using this model with a R^2 of 0.85, although the 1-day Re isotherm curve was well fitted using Freundlich model with a R^2 of 0.99.

It is noted that without pH adjustment, the equilibrium pH value for the 6-day Re batch experiment was 10.6, which was much higher than the equilibrium pH value of 6.8 for the Tc batch experiment under similar conditions. The pH values of the Tc and Re stock solutions were ~7.0 and 8.6, respectively. The slightly higher pH of the Re stock solution could not contribute to the entire pH increase for the Re batch experiment. In a separate batch experiment using the identical setup for obtaining the Re isotherm curve, the pH value of each test tube was measured daily. As shown in Fig. S3, with the initial Re concentration of 5×10^{-5} M, the pH value increased from 6.62 to 7.41 over the first day and then remained within ±0.1 unit, while for the other samples with the initial Re concentration of 1.25×10^{-4} - 5×10^{-3} M, the pH value increased from 6.76-7.41 to ~10.00 during the first day and then gradually increased to ~10.44 at the end of the 6-day experiment. This pH variation for the Re batch experiments was not understood, which may need further investigation.

To understand if and how the main metal ions in AGW might influence Re removal by pFe, Na, K, Ca and Mg concentrations in the effluents after pFe was in contact with 5×10^{-5} M ReO_4^-

in AGW for 6 days were analyzed and compared to the concentrations of these ions in initial AGW. As shown in Table S1, with a solid/liquid ratio of 10 g/L, the Re removal rate was 99.7%. Na and K concentrations increased in the effluent probably due to impurities of pFe, indicating that Na and K were not bound on pFe and their effects on Re removal by pFe should be minimal. On the other hand, Ca and Mg concentrations decreased in the effluent, indicating that Ca and Mg were removed by pFe. Ca and Mg were likely incorporated into the structure of Fe_3O_4 by substituting for Fe^{2+}, a major corrosion product of pFe. The presence of Fe_3O_4 was verified by powder X-ray diffraction pattern of the pFe in contact with water for 6 days (Fig. S4) and by Fe K-edge XANES and EXAFS spectra which will be discussed below. Ca and Mg at their concentration levels in groundwater should have limited effects on Re removal by pFe, because Re and Ca/Mg don't necessarily compete for the same binding sites. However, it is unknown whether Ca and Mg at much higher concentrations will impact the Re removal by pFe in other environmental applications.

The removal capacities of the present pFe material for sequestering TcO_4^- or its surrogate, ReO_4^-, from aqueous media are compared with some ZVI based materials published in the literature (Table 1), in which the pH values and analyst concentrations used in each of these studies were included in the table for comparison. It is noted that zirconia supported nano ZVI removed ~50% (K_d = 370 mL/g) of the TcO_4^- from a pH 14 tank waste simulant containing 0.51 mM TcO_4^- through reduction, while a silica gel supported nano ZVI removed >95% TcO_4^- (K_d = 290 mL/g) from a neutral pH eluate simulant containing 0.076 mM TcO_4^- [33]. Starch-stabilized nano ZVI rapidly reduced ReO_4^- to ReO_2 at ambient temperatures and near pH values [34, 36]. Graphene supported nano ZVI was effective at removing ReO_4^- from aqueous solution with a capacity of 75 mg/g through both adsorption and reduction mechanisms at pH 3 [35]. More

recently, fresh nano ZVI was reported to be effective for removing ReO_4^- from high pH and nitrate aqueous media via the reductive precipitation to ReO_2, which indicated that the ReO_4^- removal capacity increased at pH from 4 to 7.5, and then decreased to near zero at pH 12 [37]. The Tc or Re concentration, pH and the presence of other competing ions may dramatically impact their removal capacity. As a result, batch sorption data obtained under different experimental conditions may not be directly comparable. However, by comparison, the current pFe material is among the best ZVI materials for Tc sequestration from aqueous media, as evidenced by its Tc sorption coefficient K_d value ($1.8 \pm 0.6 \times 10^6$ mL/g) and saturation removal capacity (27.5 mg/g) at the equilibrium pH values. More importantly, the pFe material is much less expensive (~$4/kg) than the nano ZVI materials, which may offer significant advantages for its widespread practical applications to TcO_4^- sequestration from groundwater or even liquid nuclear waste streams.

3.3. Chemical speciation of the removed Tc and Re

Technetium K-edge XANES (A) and EXAFS in k space (B) of two selected pFe samples exposed to TcO_4^- of different concentrations in AGW are shown in Fig. 5, in comparison with the spectra of several model samples. The preparation of model samples Tc(IV)-Fe(OOH) and Tc(IV)-Fe_3O_4 was described in literature [48].The Tc K-edge XANES data (dotted lines) of the two samples were fitted using linear combination fitting method via the use of Athena [46]. The fits are shown as green and red curves in Fig. 5, and the obtained fitting results are summarized in Table 2. The Tc XANES fitting results consistently demonstrated that for both samples, TcO_4^- was 20-30%, the total Tc(IV) associated with Fe(OOH) and Fe_3O_4 was 70-80%, and TcO_2 was <7%, which is within the error of the linear combination fitting method [46]. The Tc EXAFS data of these two samples were also fitted using these model samples (Fig. 5B), which indicated

that 70-80% of the Tc species were associated with Fe(OOH) and Fe_3O_4, and the other 20-30% of the Tc species was TcO_4^-. The presence of Fe(OOH) and Fe_3O_4 was verified by the power X-ray diffraction pattern of pFe in contact with water for 6 days under ambient conditions (Fig. S4).

The Re L-edge XANES spectra of pFe after exposure to ReO_4^- in AGW are shown in Fig. 6A, in comparison with the spectra of two standards, sodium perrhenate ($NaReO_4$) and Re oxide (ReO_2) [49-52]. The L-edge absorption peaks of the pFe exposed to ReO_4^- were at 10534.8 eV, with another peak at about 10546.1 eV. Linear combination fitting indicated that all the Re associated with the pFe was ReO_4^-. Thus, graphical comparison and linear combination fitting clearly indicated that the sequestered Re species on pFe in AGW at an equilibrium pH of 10.6 was ReO_4^-, without detectable ReO_2.

Rhenium L-edge EXAFS spectra in k-space and Fourier transform plots in R magnitude of pFe after exposure to ReO_4^- are shown in Fig. 6B and 6C, respectively, together with the two standards. The experimental data are shown as dotted lines, and EXAFS fits are shown as colored lines. The fitted EXAFS parameters of these samples are summarized in Table 3. The EXAFS spectrum of $NaReO_4$ was fitted by tetrahedral Re-O path with Re-O distance of 1.728 Å [47], obtaining the fitted Re-O distance of 1.731 Å and a coordination number of 2.8, smaller than 4. Including the second Re-O path (R = 3.06 Å) slightly improved the fitting statistics. However, the Re-Na scattering paths with Re-Na distances of 3.794 and 3.975 Å were not included in EXAFS data fitting, because the EXAFS signal was too weak beyond 3 Å. Like $NaReO_4$, the Re L-edge EXAFS data of pFe exposed to ReO_4^- were fitted with tetrahedral Re-O paths at a Re-O distance of 1.715 ± 0.003 Å with a coordination number of 2.6 ± 0.3, very similar to those of $NaReO_4$. Including the second Re-O path also slightly improved their fitting statistics. However, no meaningful Re-Fe scattering was observed to elucidate interaction

between ReO_4^- and the substrate. The EXAFS data fitting of the pFe, as well as $NaReO_4$, was good as measured by the reduced χ^2 of 28 (Table 3). Thus, the Re L-edge EXAFS spectra of pFe exposed to ReO_4^- were visibly identical to those of $NaReO_4$, but drastically different from those of ReO_2 (Fig. 6B and 6C). These results confirmed that the Re species associated with pFe was ReO_4^-, rather than its reduced ReO_2. While our results are different from previous reports regarding Re speciation on ZVI [35, 37], they are consistent with Re speciation (i.e., ReO_4^- >90%) on steel coupon that is exposed to $KReO_4$ solution [53]. It is not entirely clear why different Re speciation is observed on iron materials exposed to ReO_4^- among these studies, but it is likely related to differences in solution chemistry and batch experimental conditions.

3.4. Tc and Re stabilization by pFe

To further understand the mechanisms responsible for Tc and Re sequestration and stabilization, Fe K-edge XANES (A) and EXAFS in k space (B) of pFe before and after exposure to ReO_4^- are shown in Fig. 7, in comparison with two standards, metal iron and Fe(OOH). Linear combination fitting was conducted to analyze the experimental Fe K-edge XANES and EXAFS spectra of this pFe sample using Athena, as shown in Fig. 7. The Fe K-edge XANES fitting gave 85% pFe and 15% Fe(OOH), while the Fe EXAFS fitting gave 78% pFe and 22% Fe(OOH). Consistently both Fe K-edge XANES and EXAFS spectra demonstrated that the pFe sample after Re removal from AGW at pH value of 10.6 was characterized primarily by pFe (~80%) and secondarily by Fe(OOH) (~20%). These results further demonstrate that pFe corroded and Fe(OOH), and possibly Fe_3O_4, formed on pFe surfaces during this six-day batch experiment. It is expected that such corrosion of pFe would be more significant for the Tc sequestration experiment at pH 6.8 under, otherwise, similar experimental conditions [36], because H^+ facilitates the oxidation of Fe^0 to Fe^{2+} in water.

In order to further understand Re speciation and immobilization mechanisms, an extraction experiment for Re using sodium sulfate and potassium iodate, as well as deionized water, was conducted. Fig. 8 shows that with one-minute Vortex agitation, the extraction percentage of Re species by deionized water increased to 2.8%, compared to 1.25% for deionized water extraction without agitation. The extraction percentages of Re species by 0.1 M Na_2SO_4 and even 1 M KI solution were similar, just ~2%. Considering similar chemistries between ReO_4^- and TcO_4^-, the results demonstrated that the sequestered ReO_4^- species was unlikely adsorbed on pFe as an outer-sphere complex, in contrast to TcO_4^- on organoclay and activated carbon, which is desorbed by 1 M KI solution at levels of 95.6% and 86.1%, respectively [54]. Instead, these results confirmed that the Re species was likely co-precipitated with Fe(OOH) and Fe_3O_4, so that it was not ion-exchanged by other anions.

Thus, for sequestration of TcO_4^- by pFe at a pH of ~6.8, 70-80% of the spiked TcO_4^- was reduced to Tc(IV) that was further incorporated into Fe corrosion products (i.e., Fe(OOH), Fe_3O_4) [21, 24, 48, 55]. The remaining 20-30% of TcO_4^- remained unreduced, which was more likely incorporated into the structure of Fe corrosion products [53], rather than adsorbed on pFe or its corrosion products as an outer-sphere complex [54]. In contrast, for sequestration of ReO_4^- by pFe at a pH of ~10.6, ReO_4^- was not reduced under similar ambient oxic conditions, because ReO_4^- has higher redox potential (E^0 = -0.548 V) than that for TcO_4^- (E^0 = -0.361 V) [36]. Meanwhile, ReO_4^- sequestered by pFe was not significantly extracted (<2%) by 1 M KI solution. Thus, the sequestration of ReO_4^- and by chemical analogy, unreduced TcO_4^-, by pFe is likely through incorporation into the structure of Fe corrosion products (i.e., Fe(OOH), Fe_3O_4). These results are consistent with several of previous studies [24, 48, 55], but in contrast with some other studies that have proposed the chemical reduction of TcO_4^- to TcO_2 [33] or ReO_4^- to ReO_2

[34-37]. In addition, while the Tc(IV) incorporation into α-Fe_2O_3 has been demonstrated by quantum mechanical calculation [56], the incorporation of TcO_4^- or ReO_4^- into the corrosion products warrants further investigation.

4. Conclusions

A novel material, pFe, was developed and evaluated for TcO_4^- sequestration from simulated contaminated groundwater and liquid nuclear waste streams. The pFe material was significantly more effective than gFe at removing TcO_4^- and ReO_4^- from groundwater under oxic conditions. While gFe removes very little TcO_4^- or ReO_4^- from AGW at pH ≥ 6 under ambient oxic conditions, the pFe effectively sequesters TcO_4^- or ReO_4^- from AGW under similar oxic conditions, with a capacity of 27.5 mg Tc/g pFe at pH ~6.8, and a capacity of 23.9 mg Re/g pFe at pH ~10.6. Our results indicate that the pFe is more effective for TcO_4^- sequestration than for ReO_4^- removal, which is probably related to the lower redox potential of $TcO_4^-$and lower pH values in the Tc experiments. If redox processes play a role in TcO_4^- removal, additional caution is required for the use of ReO_4^- as a TcO_4^- surrogate. In addition, pFe can effectively sequester TcO_4^- from contaminated aqueous media through the incorporation of Tc(IV)) and/or TcO_4^- into the structure of the Fe corrosion products (i.e., Fe(OOH), Fe_3O_4) [24], which greatly reduces the risk of remobilization [21]. More importantly, the sequestration of TcO_4^- from aqueous media by pFe occurs under ambient oxic conditions, with no need to create and maintain chemically reducing conditions. Therefore, inexpensive and high-capacity pFe materials may provide a practical solution for removing $^{99}TcO_4^-$ and other anionic contaminants from environmental systems and liquid nuclear wastes. Future efforts may focus on improved methodologies (e.g., special additives, sonication, acid washing, reduction of particle size) for producing porous iron materials with even higher surface areas to further increase the capacity for TcO_4^- sequestration.

Acknowledgements

This work was supported by the Laboratory Directed Research and Development (LDRD) program (Grant No.: LDRD-2017-00014) within the Savannah River National Laboratory (SRNL). Work was conducted at SRNL under the U.S. Department of Energy Contract DE-AC09-96SR18500. Dr. Seaman's participation was supported by the U. S. Department of Energy under Award Numbers DE-FC09-07SR22506 to the University of Georgia Research Foundation. This research used resources (Sector 20) of the Advanced Photon Source, an Office of Science User Facility operated for the U.S. Department of Energy (DOE) Office of Science by Argonne National Laboratory under Contract No. DE-AC02-06CH11357. The Sector 20 operations were also supported by the Canadian Light Source (CLS) and its funding partners. This research also used VESPERS beamline of the CLS that was supported by the NSERC of Canada, the NRC of Canada, the Canadian Institutes of Health Research, and the Province of Saskatchewan. We greatly appreciate Dr. Yongfeng Hu at CLS for providing Fe K-edge data of metal iron and Fe(OOH), and Dr. Steve Heald at Advanced Photo Source for provision of Tc K-edge data of several model samples.

References

[1] J.P. Icenhower, N.P. Qafoku, J.M. Zachara, W.J. Martin, The biogeochemistry of technetium: A review of the behavior of an artificial element in the natural environment, Am. J. Sci., 310 (2010) 721-752.
[2] A.H. Meena, Y. Arai, Environmental geochemistry of technetium, Environ. Chem. Lett., 15 (2017) 241-263.
[3] J.L. Kloosterman, Nuclear Waste Production, www.\technetium\homepage [Online], 2008.
[4] M.M. Valenta, K.E. Parker, E.M. Pierce, Tc-99 Ion Exchange Resin Testing, PNNL-19681, Pacific Northwest National Laboratory, Richland, Washington 99352, 2010.
[5] B.H. Gu, K.E. Dowlen, L.Y. Liang, J.L. Clausen, Efficient separation and recovery of technetium-99 from contaminated groundwater, Sep. Technol., 6 (1996) 123-132.
[6] L.Y. Liang, B.H. Gu, X.P. Yin, Removal of technetium-99 from contaminated groundwater with sorbents and reductive materials, Sep. Technol., 6 (1996) 111-122.
[7] J.M. McBeth, J.R. Lloyd, G.T.W. Law, F.R. Livens, I.T. Burke, K. Morris, Redox interactions of technetium with iron-bearing minerals, Mineral. Mag., 75 (2011) 2419-2430.

[8] A.E. Plymale, J.K. Fredrickson, J.M. Zachara, A.C. Dohnalkova, S.M. Heald, D.A. Moore, D.W. Kennedy, M.J. Marshall, C.M. Wang, C.T. Resch, P. Nachimuthu, Competitive reduction of pertechnetate ((TcO_4^-)-Tc-99) by dissimilatory metal reducing bacteria and biogenic Fe(II), Environ. Sci. Technol., 45 (2011) 951-957.
[9] E.M. Pierce, R.J. Serne, W. Um, S.V. Mattigod, J.P. Icenhower, N.P. Qafoku, J. Westsik, J.H., R.D. Scheele, Review of Potential Candidate Stabilization Technologies for Liquid and Solid Secondary Waste Streams, PNNL-19122, Pacific Northwest National Laboratory, Richland, Washington 99352, 2010.
[10] W.M. Wu, J. Carley, T. Gentry, M.A. Ginder-Vogel, M. Fienen, T. Mehlhorn, H. Yan, S. Caroll, M.N. Pace, J. Nyman, J. Luo, M.E. Gentile, M.W. Fields, R.F. Hickey, B.H. Gu, D. Watson, O.A. Cirpka, J.Z. Zhou, S. Fendorf, P.K. Kitanidis, P.M. Jardine, C.S. Criddle, Pilot-scale in situ bioremedation of uranium in a highly contaminated aquifer. 2. Reduction of U(VI) and geochemical control of U(VI) bioavailability, Environ. Sci. Technol., 40 (2006) 3986-3995.
[11] D.B. Watson, W.M. Wu, T. Mehlhorn, G.P. Tang, J. Earles, K. Lowe, T.M. Gihring, G.X. Zhang, J. Phillips, M.I. Boyanov, B.P. Spalding, C. Schadt, K.M. Kemner, C.S. Criddle, P.M. Jardine, S.C. Brooks, In situ bioremediation of uranium with emulsified vegetable oil as the electron donor, Environ. Sci. Technol., 47 (2013) 6440-6448.
[12] D. Li, K. D.I., Solubility of Technetium Dioxides (TcO_2-c, $TcO_2 \cdot 1.6H_2O$ and $TcO_2 \cdot 2H_2O$) in Reducing Cementitious Material Leachates: A Thermodynamic Calculation, Savannah River National Laboratory, 2012.
[13] J.K. Fredrickson, J.M. Zachara, A.E. Plymale, S.M. Heald, J.P. McKinley, D.W. Kennedy, C.X. Liu, P. Nachimuthu, Oxidative dissolution potential of biogenic and ablogenic TcO_2 in subsurface sediments, Geochim. Cosmochim. Acta, 73 (2009) 2299-2313.
[14] J.M. McBeth, G. Lear, J.R. Lloyd, F.R. Livens, K. Morris, I.T. Burke, Technetium reduction and reoxidation in aquifer sediments, Geomicrobiol. J., 24 (2007) 189-197.
[15] R.M. Asmussen, C.I. Pearce, B.W. Miller, A.R. Lawter, J.J. Neeway, W.W. Lukens, M.E. Bowden, M.A. Miller, E.C. Buck, R.J. Serne, N.P. Qafoku, Getters for improved technetium containment in cementitious waste forms, J. Hazard. Mater., 341 (2018) 238-247.
[16] C.I. Pearce, J.P. Icenhower, R.M. Asmussen, P.G. Tratnyek, K.M. Rosso, W.W. Lukens, N.P. Qafoku, Technetium stabilization in low-solubility sulfide phases: A review, ACS: Earth Space Chem., 2 (2018) 532-547.
[17] Y. Liu, J. Terry, S. Jurisson, Pertechnetate immobilization in aqueous media with hydrogen sulfide under anaerobic and aerobic environments, Radiochim. Acta, 95 (2007) 717-725.
[18] Y. Liu, J. Terry, S. Jurisson, Pertechnetate immobilization with amorphous iron sulfide, Radiochim. Acta, 96 (2008) 823-833.
[19] D.M. Fan, R.P. Anitori, B.M. Tebo, P.G. Tratnyek, J.S.L. Pacheco, R.K. Kukkadapu, M.H. Engelhard, M.E. Bowden, L. Kovarik, B.W. Arey, Reductive sequestration of pertechnetate ((TcO_4^-)-Tc-99) by nano zerovalent iron (nZVI) transformed by abiotic sulfide, Environ. Sci. Technol., 47 (2013) 5302-5310.
[20] D.M. Fan, R.P. Anitori, B.M. Tebo, P.G. Tratnyek, J.S.L. Pacheco, R.K. Kukkadapu, L. Kovarik, M.H. Engelhard, M.E. Bowden, Oxidative remobilization of technetium sequestered by sulfide-transformed nano zerovalent iron, Environ. Sci. Technol., 48 (2014) 7409-7417.
[21] W. Um, H.S. Chang, J.P. Icenhower, W.W. Lukens, R.J. Serne, N.P. Qafoku, J.H. Westsik, E.C. Buck, S.C. Smith, Immobilization of 99-technetium (VII) by Fe(II)-goethite and limited reoxidation, Environ. Sci. Technol., 45 (2011) 4904-4913.
[22] E.M. Pierce, K. Lilova, D.M. Missimer, W.W. Lukens, L.L. Wu, J. Fitts, C. Rawn, A. Huq, D.N. Leonard, J.R. Eskelsen, B.F. Woodfield, C.M. Jantzen, A. Navrotsky, Structure and thermochemistry of perrhenate sodalite and mixed guest perrhenate/pertechnetate sodalite, Environ. Sci. Technol., 51 (2017) 997-1006.
[23] J.O. Dickson, J.B. Harsh, W.W. Lukens, E.M. Pierce, Perrhenate incorporation into binary mixed sodalites: The role of anion size and implications for technetium-99 sequestration, Chem. Geol., 395 (2015) 138-143.

[24] J. Liu, C.I. Pearce, O. Qafoku, E. Arenholz, S.M. Heald, K.M. Rosso, Tc(VII) reduction kinetics by titanomagnetite (Fe3-xTixO4) nanoparticles, Geochim. Cosmochim. Acta, 92 (2012) 67-81.
[25] R.A. Crane, T.B. Scott, Nanoscale zero-valent iron: Future prospects for an emerging water treatment technology, J. Hazard. Mater., 211 (2012) 112-125.
[26] S.M. Ponder, J.G. Darab, T.E. Mallouk, Remediation of Cr(VI) and Pb(II) aqueous solutions using supported, nanoscale zero-valent iron, Environ. Sci. Technol., 34 (2000) 2564-2569.
[27] J.A. Lackovic, N.P. Nikolaidis, G.M. Dobbs, Inorganic arsenic removal by zero-valent iron, Environ. Eng. Sci., 17 (2000) 29-39.
[28] A. Agrawal, P.G. Tratnyek, Reduction of nitro aromatic compounds by zero-valent iron metal, Environ. Sci.Technol., 30 (1996) 153-160.
[29] B. Gu, L. Liang, M.J. Dickey, X. Yin, S. Dai, Reductive precipitation of uranium(VI) by zero-valent iron, Environ. Sci. Technol., 32 (1998) 3366-3373.
[30] B. Calderon, A. Fullana, Heavy metal release due to aging effect during zero valent iron nanoparticles remediation, Water Res., 83 (2015) 1-9.
[31] X.H. Guan, Y.K. Sun, H.J. Qin, J.X. Li, I.M.C. Lo, D. He, H.R. Dong, The limitations of applying zero-valent iron technology in contaminants sequestration and the corresponding countermeasures: The development in zero-valent iron technology in the last two decades (1994-2014), Water Res., 75 (2015) 224-248.
[32] K.J. Cantrell, D.I. Kaplan, T.W. Wietsma, Zero-valent iron for the in-situ remediation of selected metals in groundwater, J. Hazard. Mater., 42 (1995) 201-212.
[33] J.G. Darab, A.B. Amonette, D.S.D. Burke, R.D. Orr, S.M. Ponder, B. Schrick, T.E. Mallouk, W.W. Lukens, D.L. Caulder, D.K. Shuh, Removal of pertechnetate from simulated nuclear waste streams using supported zerovalent iron, Chem. Mater., 19 (2007) 5703-5713.
[34] Q.W. Ding, T.W. Qian, F. Yang, H.F. Liu, L.X. Wang, D.Y. Zhao, M.G. Zhang, Kinetics of Reductive Immobilization of Rhenium in Soil and Groundwater Using Zero Valent Iron Nanoparticles, Environ. Eng. Sci., 30 (2013) 713-718.
[35] J. Li, C.L. Chen, R. Zhang, X.K. Wang, Reductive immobilization of Re(VII) by graphene modified nanoscale zero-valent iron particles using a plasma technique, Sci. China-Chem., 59 (2016) 150-158.
[36] H.F. Liu, T.W. Qian, D.Y. Zhao, Reductive immobilization of perrhenate in soil and groundwater using starch-stabilized ZVI nanoparticles, Chinese Sci. Bull., 58 (2013) 275-281.
[37] B.A. Lenell, Y. Arai, Perrhenate sorption kinetics in zerovalent iron in high pH and nitrate media, J. Hazard. Mater., 321 (2017) 335-343.
[38] B.J. Allred, Laboratory evaluation of porous iron composite for agricultural drainage water filter treatment, Trans. Am. Soc. Agr. Biol. Eng., 55 (2012) 683-1697.
[39] J.C. Seaman, E. Dorward, J. Cochran, Effectiveness of Porous Iron Composite (PIC) Materials for Removing Radionuclides from Low Quality Groundwater: Batch and Column Test Results, Savannah River Ecology Laboratory, The University of Georgia, Aiken, SC 29802, 2015.
[40] J.G. Darab, P.A. Smith, Chemistry of technetium and rhenium species during low-level radioactive waste vitrification, Chem. Mater., 8 (1996) 1004-1021.
[41] R.N. Strom, D.S. Kaback, SRP Baseline Hydrogeologic Investigation: Aquifer Cheracterization. Groundwater Geochemistry of the Savannah River Site and Vicinity, WSRC-RP-92-450, Westinghouse Savannah River Company, Environmental Sciences Section, Aiken, SC, 1992.
[42] D. Li, D.I. Kaplan, K.A. Roberts, J.C. Seaman, Mobile colloid generation induced by a cementitious plume: mineral surface-charge controls on mobilization, Environ. Sci. Technol., 46 (2012) 2755-2763.
[43] M.E. Stallings, M.J. Barnes, T.B. Peters, D.P. Diprete, F.F. Fondeur, D.T. Hobbs, S.D. Fink, Characterization of Supernate Samples from High Level Waste Tanks 13H, 30H, 37H, 39H, 45F, 46F and 49H, WSRC-TR-2004-00386 Revision 2, Westinghouse Savannah River Company, Aiken, SC 29808, 2004.
[44] USEPA, Method 6020A, Rev. 0. Inductively coupled plasma-mass spectrometry. , in: Test Methods for Evaluating Solid Waste, Physical/Chemical Methods (SW-846) Office of Solid Waste, Washington, DC, 2007.

[45] R.F. Feng, W. Dolton, R. Igarashi, G. Wright, M. Bradford, S. McIntyre, Commissioning of the VESPERS Beamline at the Canadian Light Source, AIP Conf. Proc., 1234 (2010) 315-318.
[46] B. Ravel, M. Newville, Athena, Artemis, Hephaestus: data analysis for X-ray absorption spectroscopy using IFEFFIT, J. Synchrotron Radiat., 12 (2005) 537−541.
[47] A. Atzesdorfer, K.J. Range, Sodium metaperrhenate, NaReO4 - High-pressure synthesis of single-crystals and structure refinement, Zeit. Naturf. Sect. B-J. Chem. Sci., 50 (1995) 1417-1418.
[48] T. Peretyazhko, J.M. Zachara, S.M. Heald, B.H. Jeon, R.K. Kukkadapu, C. Liu, D. Moore, C.T. Resch, Heterogeneous reduction of Tc(VII) by Fe(II) at the solid-water interface, Geochim. Cosmochim. Acta, 72 (2008) 1521-1539.
[49] G.Y. Yurkov, A.V. Kozinkin, Y.A. Koksharov, A.S. Fionov, N.A. Taratanov, V.G. Vlasenko, I.V. Pirog, O.N. Shishilov, O.V. Popkov, Synthesis and properties of rhenium-polyethylene nanocomposite, Composites Part B-Eng., 43 (2012) 3192-3197.
[50] F. Poineau, M. Fattahi, B. Grambow, Correlation between X-ray chemical shift and partial charge in Tc(IV) complexes: Determination of Tc partial charge in TcnOy(4n-2y)+, Radiochim. Acta, 94 (2006) 559-563.
[51] A. Tougerti, S. Cristol, E. Berrier, V. Briois, C. La Fontaine, F. Villain, Y. Joly, XANES study of rhenium oxide compounds at the L-1 and L-3 absorption edges, Phys. Rev. B, 85 (2012), Article Number: 125136.
[52] J. Yi, J.T. Miller, D.Y. Zemlyanov, R.H. Zhang, P.J. Dietrich, F.H. Ribeiro, S. Suslov, M.M. Abu-Omar, A Reusable Unsupported Rhenium Nanocrystalline Catalyst for Acceptorless Dehydrogenation of Alcohols through gamma-C-H Activation, Angew. Chem. Internat. Ed., 53 (2014) 833-836.
[53] S.M. Heald, K.M. Krupka, C.F. Brown, Incorporation of pertechnetate and perrhenate into corroded steel surfaces studied by X-ray absorption fine structure spectroscopy, Radiochim. Acta, 100 (2012) 243-253.
[54] D. Li, J.C. Seaman, D.I. Kaplan, S.M. Heald, C.J. Sun, Pertechnetate (TcO_4^-) sequestration from groundwater by cost-effective organoclays and granular activated carbon under oxic environmental conditions, Chem. Eng. J., 360 (2019) 1-9.
[55] W. Um, H. Chang, J.P. Icenhower, W.W. Lukens, R.J. Serne, N. Qafoku, R.K. Kukkadapu, J.H. Westsik, Iron oxide waste form for stabilizing Tc-99, J. Nucl. Mater., 429 (2012) 201-209.
[56] F.N. Skomurski, K.M. Rosso, K.M. Krupka, B.P. McGrail, Technetium incorporation into hematite (alpha-Fe_2O_3), Environ. Sci. Technol., 44 (2010) 5855-5861.
[57] R.W.G. Wyckoff, Crystal Structure, Second Edition, Interscience Publishers, , New York, 1963.

Table 1
Comparison of porous iron (pFe) with several reported ZVI-based materials for TcO_4^- or ReO_4^- removal from aqueous media.

ZVI materials	Aqueous media	pH	Sorbate	Sorption coefficient, K_d (mL/g) [a]	Removal capacity (mg/g) [a]	Removal mechanism	References
Nano ZVI on zirconia	Waste simulant	14	5.1×10^{-4} M TcO_4^-	370		Reduction	[33]
Nano ZVI on silica	Eluate simulant	~7	7.6×10^{-5} M TcO_4^-	290		Reduction	
Nano ZVI on starch	Water	7	4×10^{-5} M ReO_4^-	658		Reduction	[34]
Nano ZVI on starch	Water	7.6	4×10^{-5} M ReO_4^-	74		Reduction	[36]
Nano ZVI on graphene	Water	3	1.4×10^{-4} M ReO_4^-	2143	75	Adsorption / reduction	[35]
Nano ZVI	Salt solution	4	2.7×10^{-4} M ReO_4^-	239	7.5	Reduction	[37]
		7.5		547	11.6		
		10		265	8.0		
		12		0	0		
Steel coupon	Groundwater	7.4	1×10^{-4} M TcO_4^-			Reduction / co-precipitation	[53]
		7.4	1×10^{-3} M ReO_4^-			Little reduction / Co-precipitation	
gFe	Groundwater	~6	6.1×10^{-5} M TcO_4^-	3.2 ± 1.8	0.02		This work
		6.7	6×10^{-5} M ReO_4^-	12.0	0.14		
pFe	Groundwater	~6	6.1×10^{-5} M TcO_4^-	$1.8 \pm 0.6 \times 10^6$	0.61		
		6.7	6×10^{-5} M ReO_4^-	$5.4 \pm 3.1 \times 10^3$	1.09		
		6.8	Varied, TcO_4^-		27.5 [b]	Reduction / co-precipitation	
		10.6	Varied, ReO_4^-		23.9 [b]	Co-precipitation	

[a] The sorption coefficient, K_d (mL/g) and removal capacity values from the references were calculated / estimated based on the figures presented in each original publication.
[b] The Tc or Re removal capacity (mg/g) data were saturation capacities obtained from Langmuir modeling to experimental isotherm curves.

Table 2
Speciation of the removed Tc on pFe samples obtained from linear combination fitting (LCF) of Tc K-edge XANES data.[a]

Samples	TcO_4^-	Tc(IV)-Fe(OOH)	Tc(IV)-Fe_3O_4	TcO_2
pFe-1	21.0	22.8	49.2	7.0
pFe-2	27.2	19.7	51.9	1.2
[a] The errors from the XANES LCF are estimated to be ±10% [46].				

Table 3
Re L-edge EXAFS fitting data for Re species sequestered on pFe.

Samples [a]	pH	Scattering path	Interatomic distance (Å)	Coordination number	Debye–Waller factor, σ^2 (Å^2)	R-factor	Reduced χ^2
pFe_Re-6	10.6	Re-O1	1.717 ± 0.010	2.6 ± 0.3	0.0029 ± 0.0015	0.0089	27.7
$NaReO_4$	EXAFS	Re-O1	1.731 ± 0.007	2.8 ± 0.3	0.0028 ± 0.0009	0.0038	19.5
		Re-O2	3.037 ± 0.074	4	0.0314 ± 0.0163		
	X-ray structure [47]	Re-O1	1.728	4			
		Re-O2	3.06	4			
ReO_2	EXAFS	Re-O1	2.02 ± 0.02	4.5	0.0068 ± 0.0025	0.0155	71.3
		Re-Re	2.55 ± 0.03	2	0.0098 ± 0.0053		
		Re-O3	3.09 ± 0.01	2	0.0055 ± 0.0085		
		Re-Re2	3.78 ± 0.03	8	0.0102 ± 0.0029		

[a] Amplitude was set to 0.8.

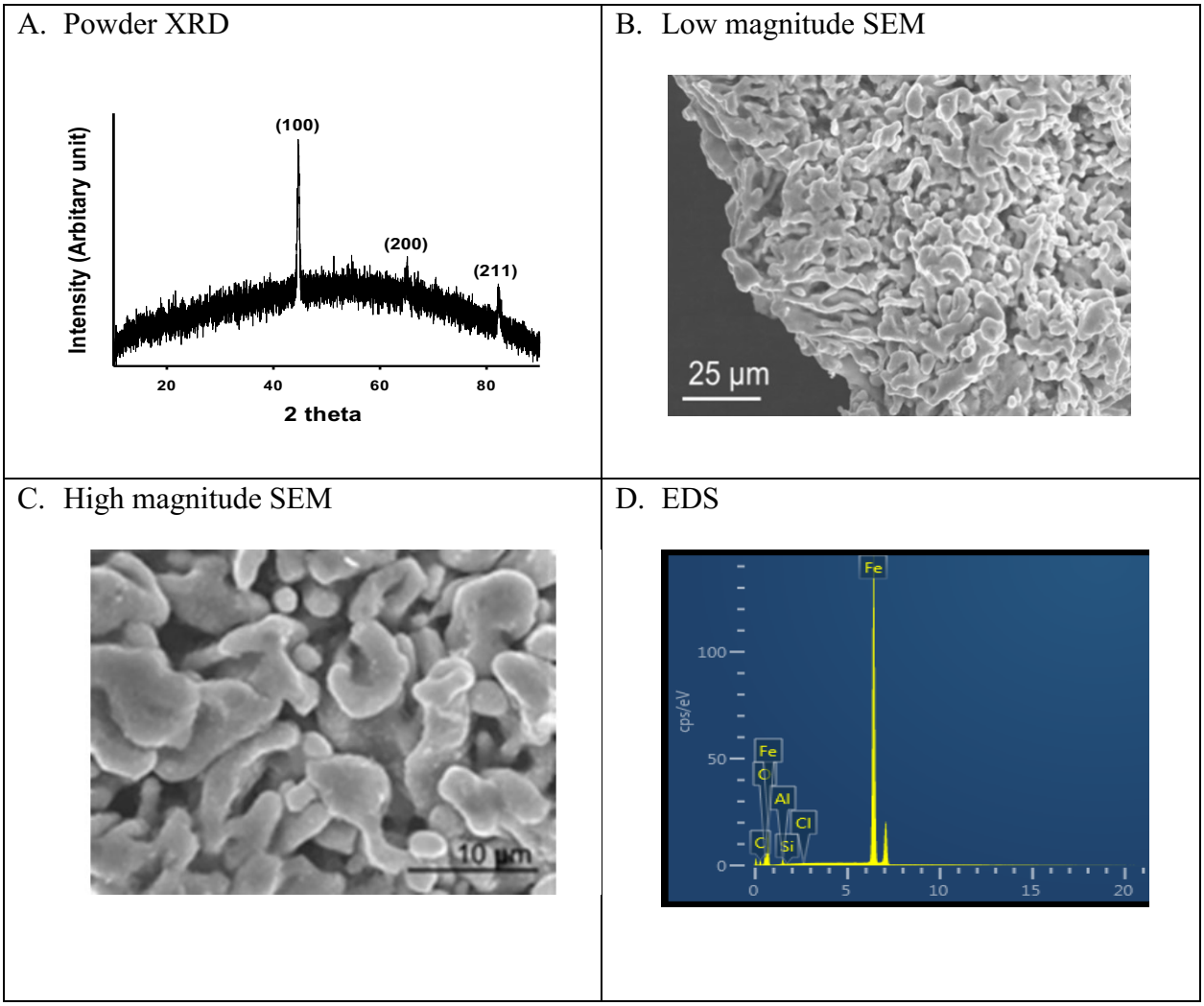

Fig. 1. Powder XRD pattern (A), SEM images (B and C) and EDS spectrum (D) of pFe.

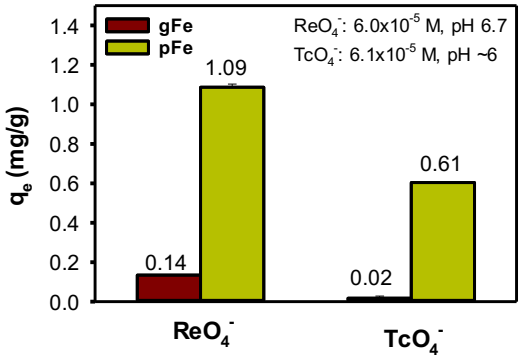

Fig. 2. Comparison of porous iron (pFe) and granular iron (gFe) for TcO_4^- and ReO_4^- removal from groundwater under oxic conditions. It is noted that for the ReO_4^- experiment, the initial Re concentration was 6.0×10^{-5} M, the sorbent loading was 10 g/L, and pH ~6.7, while for the TcO_4^- experiment, the initial Tc concentration was 6.1×10^{-5} M, the sorbent loading was 10 g/L, and pH ~6.0. Error bars represent standard deviation of 2 replicates.

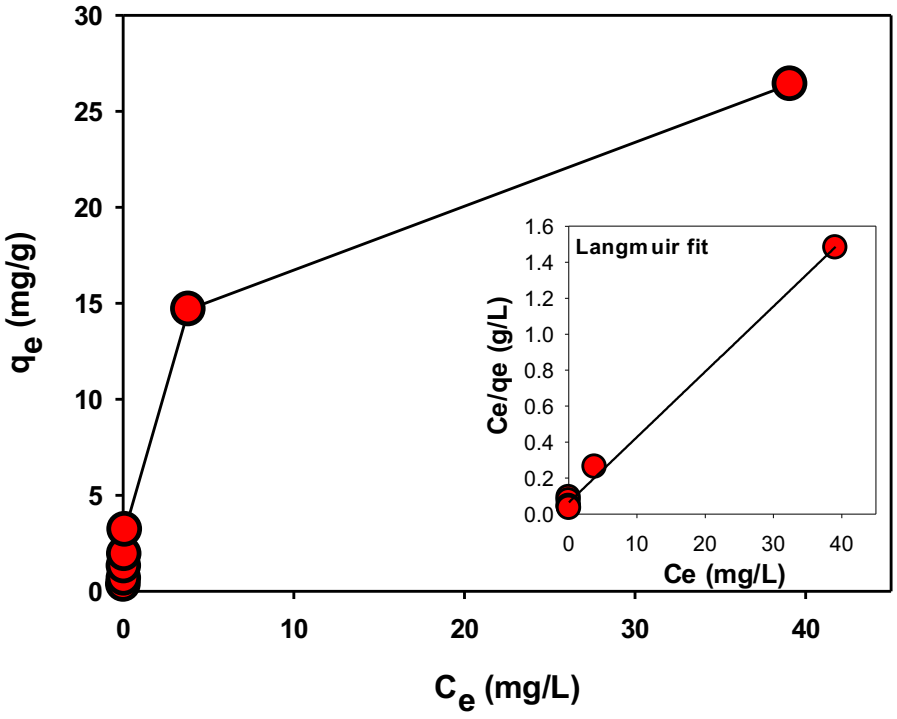

Fig. 3. Adsorption isotherm of TcO_4^- on pFe in AGW at pH ~6.8. Langmuir fit to the TcO_4^- adsorption data is shown in the inset. All measurements represent the average of two replicates, except for the data point at C_e = 39.1 mg/L.

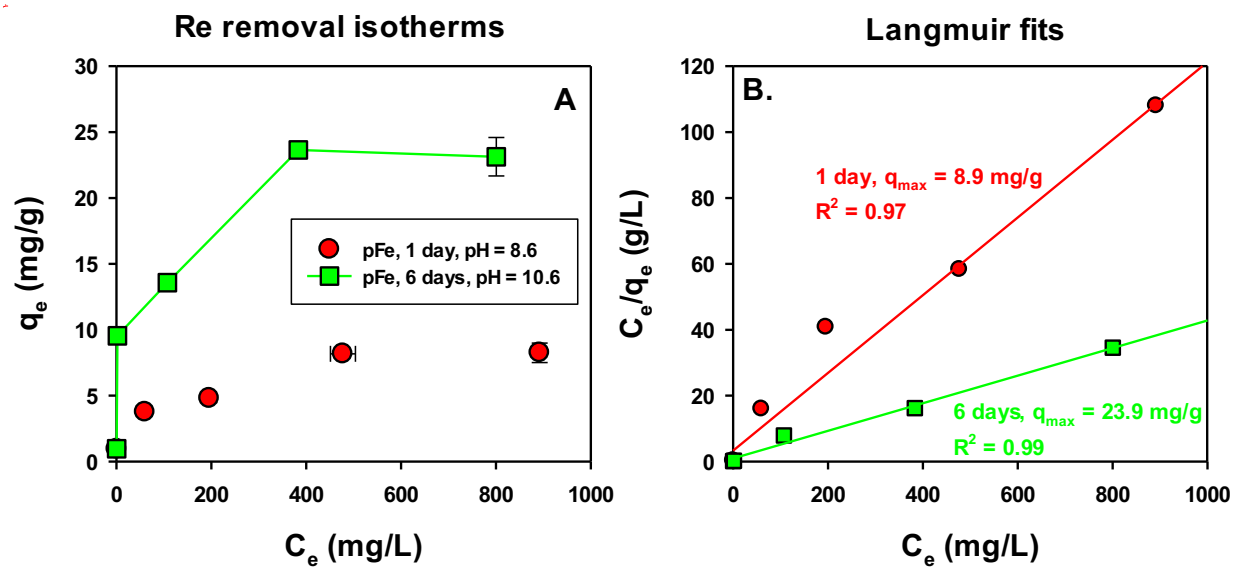

Fig. 4. Adsorption isotherms of ReO_4^- on pFe after equilibration for 1 day and 6 days (A). Langmuir fits to the adsorption data for ReO_4^- on pFe are shown at right (B). All measurements represent the average of two replicates.

A. XANES B. EXAFS in K

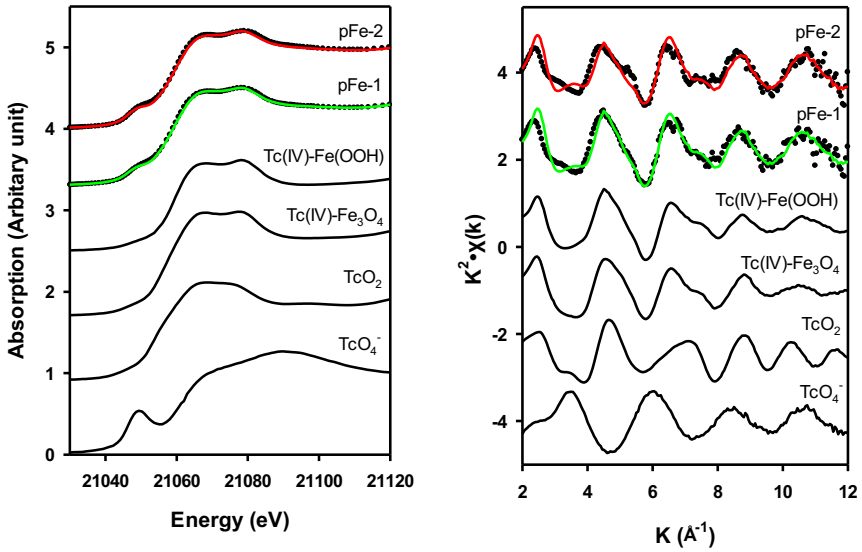

Fig. 5. Tc K-edge XANES (A) and EXAFS in k space (B) of pFe exposed to TcO_4^- in artificial groundwater, in comparison with Tc K-edge data of several model samples. Samples pFe-1 and pFe-2 were the same porous iron exposed to TcO_4^- of different concentrations. The green and red curves were linear combination fits to the experimental data using Athena.

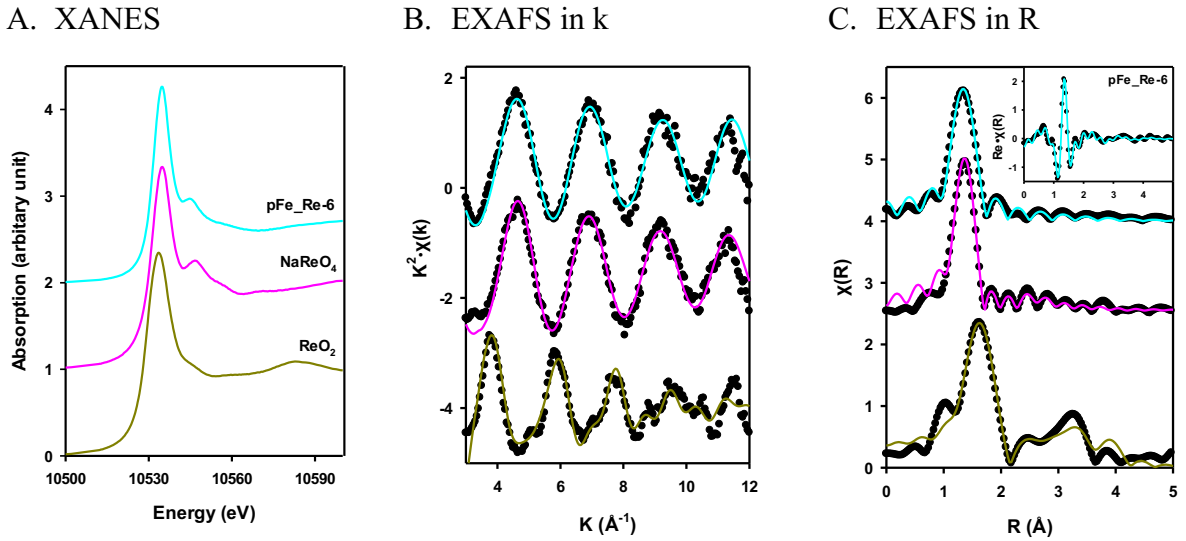

Fig. 6. Re L-edge XANES (A), EXAFS in k space (B) and EXAFS in R space (C) of Re species on pFe, in comparison with Re L-edge data of two model compounds, $NaReO_4$ and ReO_2. Fits to the Re EXAFS data of ReO_2 were made in R space (R from 1 to 3.8 Å) and obtained by taking the Fourier transform (FT) of χ(k) (k from 3.5 to 10.8) with a k weighting of 2, based on crystal structure data of ReO_2 [57]. The EXAFS data in real R space for pFe exposed to ReO_4^- is shown in the inset of Fig. 6C.

A. XANES B. EXAFS in k

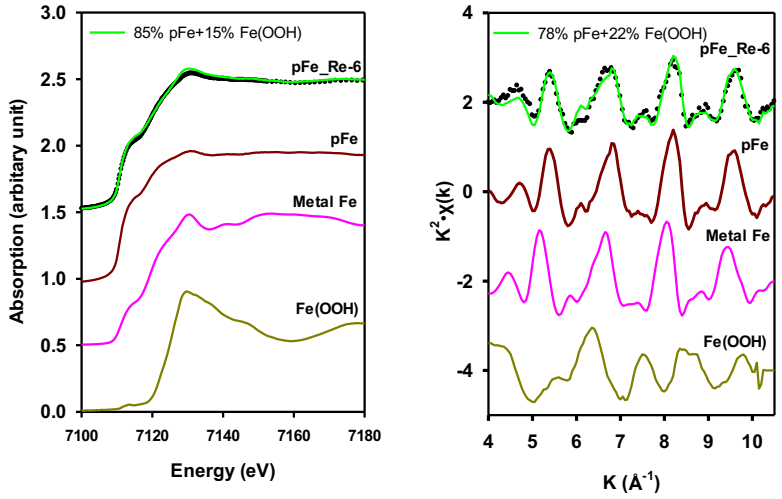

Fig. 7. Fe K-edge XANES (A) and EXAFS in k space (B) of pFe before and after exposure to ReO_4^-, in comparison with the spectra of metal iron and Fe(OOH). It is noted that the Fe K-edge spectra of our samples were collected using a fluorescence detector, while the Fe K-edge spectra of metal iron and Fe(OOH) were collected using a transmission mode.

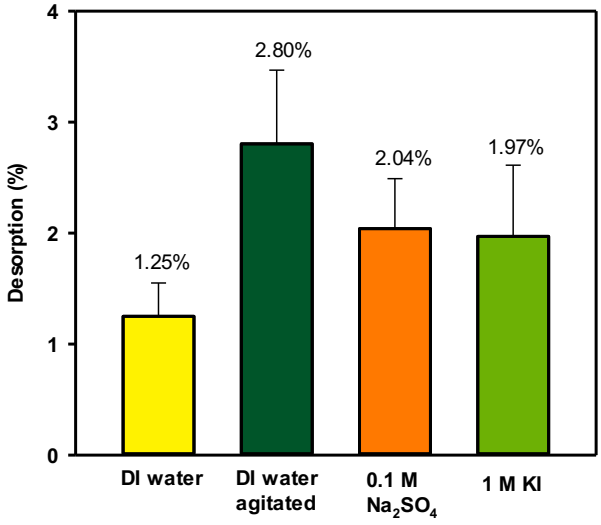

Fig. 8. Desorption of ReO_4^- on pFe by deionized (DI) water, deionized water after one-minute agitation, 0.1 M Na_2SO_4 and 1 M KI solution. The desorption batch experiment was conducted by placing the suspensions in the centrifuge tubes on a reciprocating shaker for 3 days under ambient conditions. Error bars represent standard deviation of 2 replicates.